

Radiative corrections to the Yukawa coupling constants in two Higgs doublet models

Shinya Kanemura,¹ Mariko Kikuchi,¹ and Kei Yagyu²

¹*Department of Physics, University of Toyama,*

3190 Gofuku, Toyama 930-8555, Japan

²*Department of Physics, National Central University,*

Chungli 32001, Taiwan

Abstract

We calculate one-loop corrected Yukawa coupling constants $hf\bar{f}$ for the standard model like Higgs boson h in two Higgs doublet models. We focus on the models with the softly-broken Z_2 symmetry, which is imposed to avoid the flavor changing neutral current. Under the Z_2 symmetry, there are four types of Yukawa interactions. We find that one-loop contributions from extra Higgs bosons modify the $hf\bar{f}$ couplings to be maximally about 5% under the constraint from perturbative unitarity and vacuum stability. Our results show that the pattern of tree-level deviations by the mixing effect in each type of Yukawa couplings from the SM predictions does not change even including radiative corrections. Moreover, when the gauge couplings hVV ($V = W, Z$) are found to be slightly (with a percent level) differ from the SM predictions, the $hf\bar{f}$ couplings also deviate but more largely. Therefore, in such a case, not only can we determine the type of Yukawa couplings but also we can obtain information on the extra Higgs bosons by comparing the predictions with precisely measured $hf\bar{f}$ and hVV couplings at future electron-positron colliders.

PACS numbers:

I. INTRODUCTION

By the discovery of a Higgs boson at the CERN Large Hadron Collider (LHC) [1], the standard model (SM) has been completed. So far, within the error properties of the observed boson are consistent with those of the Higgs boson in the SM such as the mass, the CP parity and the signal strengths. Thus, the discovered boson can be regarded as the SM-like Higgs boson h .

However, this fact does not necessarily mean that the SM is correct in a fundamental level, because the SM-like Higgs boson can be described not only in the minimal Higgs sector with only one isospin scalar doublet but also in non-minimal Higgs sectors. In fact, the minimal Higgs sector of the SM is nothing but an assumption without any principle. In addition, non-minimal Higgs sectors often appear in physics models beyond the SM in which several unsolved problems such as neutrino oscillation, the existence of dark matter and the baryon asymmetry of the Universe within the SM are tried to be explained. Therefore, non-minimal Higgs sectors (e.g., with additional singlets, doublets and/or triplets) should be comprehensively studied to determine the true structure of the Higgs sector and to probe new physics models.

In extended Higgs sectors, the Higgs boson coupling constants can be deviated from the corresponding SM predictions. In addition, a pattern of the deviations strongly depends on properties of the Higgs sector; i.e., the number of Higgs fields and their quantum numbers. Therefore, by “*Fingerprinting*”, i.e., by comparing the deviations in various Higgs boson couplings with the theory predictions, we can extract the structure of the Higgs sector.

The Higgs boson couplings will be measured at future colliders as precisely as possible. For example, the hVV ($V = W, Z$) and $hf\bar{f}$ ($f = t, b, \tau$) couplings are supposed to be measured with approximately 5% and 10% accuracies at the LHC with the collision energy to be 14 TeV and the integrated luminosity to be 300 fb^{-1} , respectively [2–4]. Moreover, they are expected to be measured with typically 1% at the International Linear Collider (ILC) with the collision energy to be 500 GeV and the integrated luminosity to be 500 fb^{-1} [2–5].

In this Letter, we calculate deviations in the Yukawa couplings from the SM predictions in two Higgs doublet models (THDMs) at the one-loop level, especially focusing on those for the SM-like Higgs boson h .

THDMs are a simple but well-motivated example for extended Higgs sectors. First, the electroweak rho parameter is naturally predicted to be unity at the tree level, whose experimental value is close to unity; i.e., $\rho_{\text{exp}} = 1.0004_{-0.0004}^{+0.0003}$ [6]. In the other extended Higgs sectors such as Higgs triplet models, the rho parameter is not guaranteed to be unity at the tree level. Although

even in the THDMs the rho parameter can deviate from unity due to the one-loop correction [7], its amount can easily be within the error of the measurement¹. Second, the Higgs sector in several new physics models has the structure of the THDM. For example, the supersymmetry requires at least two Higgs doublets. Neutrino mass models such as radiative seesaw models [9–12] and the neutrinophilic model [13] contain two Higgs doublet fields in their Higgs sector. The hierarchy between top and bottom quark masses may be naturally explained in the THDM [14]. Furthermore, additional CP violating phases can appear, and the strong first order electroweak phase transition can occur due to nondecoupling effects of extra scalar bosons. These characteristics are required to realize the successful electroweak baryogenesis scenario [15]. A comprehensive review of various classes of the THDM is given in Ref. [16].

Unlike the SM, in multi-doublet models, the mass matrix for fermions and the interaction matrix among a neutral Higgs boson and fermions cannot be diagonalized simultaneously. That causes flavor changing neutral currents (FCNCs) at the tree level, which are severely constrained from flavor experiments such as $K_L^0 \rightarrow \mu^+ \mu^-$, B^0 - \bar{B}^0 mixing and so on. In order to avoid the tree level FCNC, a discrete Z_2 symmetry [17] may be imposed as the simplest way. If we consider the case with the softly-broken Z_2 symmetry², there are four independent types of Yukawa interactions under the different charge assignments to quarks and charged leptons [19, 20]. We call them Type-I, Type-II, Type-X and Type-Y THDMs [21]. A lot of phenomenological studies in these THDMs have been performed before the Higgs boson discovery [22] and after that [23]. Each type of THDMs can be related to various new physics models. For example, the Higgs sector in the minimal supersymmetric SM (MSSM) corresponds to the Type-II THDM with supersymmetric relations. On the other hand, the Type-X THDM is applied to radiative seesaw models [11, 12]. Therefore, discrimination of the types of Yukawa interactions in the THDM is important to test new physics models.

In order to compare precisely measured Higgs boson couplings as mentioned above, we need to prepare precise calculations of the Higgs boson couplings in various Higgs sectors. Namely, it is essentially important to take into account the effects of radiative corrections. So far, there are several studies of one-loop calculations for the Higgs boson couplings in various versions of the THDM. One-loop corrections to the triple Higgs boson coupling hhh [24] and Yukawa couplings [25] have been calculated in the MSSM Higgs sector. In the softly-broken Z_2 symmetric THDM, the

¹ One-loop corrections to the rho parameter in Higgs triplet models have been discussed in Refs. [8].

² The unbroken, even by the vacuum, Z_2 symmetric THDM is known as the inert doublet model [18].

	Z_2 charge							Mixing factor								
	Φ_1	Φ_2	Q_L	L_L	u_R	d_R	e_R	ξ_h^u	ξ_h^d	ξ_h^e	ξ_H^u	ξ_H^d	ξ_H^e	ξ_A^u	ξ_A^d	ξ_A^e
Type-I	+	-	+	+	-	-	-	$\frac{\cos \alpha}{\sin \beta}$	$\frac{\cos \alpha}{\sin \beta}$	$\frac{\cos \alpha}{\sin \beta}$	$\frac{\sin \alpha}{\sin \beta}$	$\frac{\sin \alpha}{\sin \beta}$	$\frac{\sin \alpha}{\sin \beta}$	$\cot \beta$	$-\cot \beta$	$-\cot \beta$
Type-II	+	-	+	+	-	+	+	$\frac{\cos \alpha}{\sin \beta}$	$-\frac{\sin \alpha}{\cos \beta}$	$-\frac{\sin \alpha}{\cos \beta}$	$\frac{\sin \alpha}{\sin \beta}$	$\frac{\cos \alpha}{\cos \beta}$	$\frac{\cos \alpha}{\cos \beta}$	$\cot \beta$	$\tan \beta$	$\tan \beta$
Type-X	+	-	+	+	-	-	+	$\frac{\cos \alpha}{\sin \beta}$	$\frac{\cos \alpha}{\sin \beta}$	$-\frac{\sin \alpha}{\cos \beta}$	$\frac{\sin \alpha}{\sin \beta}$	$\frac{\sin \alpha}{\sin \beta}$	$\frac{\cos \alpha}{\cos \beta}$	$\cot \beta$	$-\cot \beta$	$\tan \beta$
Type-Y	+	-	+	+	-	+	-	$\frac{\cos \alpha}{\sin \beta}$	$-\frac{\sin \alpha}{\cos \beta}$	$\frac{\cos \alpha}{\sin \beta}$	$\frac{\sin \alpha}{\sin \beta}$	$\frac{\cos \alpha}{\cos \beta}$	$\frac{\sin \alpha}{\sin \beta}$	$\cot \beta$	$\tan \beta$	$-\cot \beta$

TABLE I: Charge assignment of the softly broken Z_2 symmetry and the mixing factors in Yukawa interactions given in Eq. (6) [21].

hhh and hVV couplings have also been calculated at the one-loop level in Ref. [26]. However, one-loop corrected Yukawa couplings have not been systematically analysed in the four types of THDMs. In this Letter, we would like to clarify how the tree level deviations in various Yukawa couplings shown in Ref. [3] can be modified by the one-loop corrections.

II. TWO HIGGS DOUBLET MODELS

In this Letter, we assume the CP-conservation of the Higgs sector. Let us fix the Z_2 charge for the two Higgs doublet fields Φ_1 and Φ_2 and the left-handed lepton-doublet and quark-doublet fields L_L and Q_L as +, -, + and +, respectively. In this set up, four types of the Yukawa interactions are defined by the choice of the Z_2 charge assignment for right-handed up-type quarks u_R , down-type quarks d_R and charged leptons e_R as listed in Table I.

The Yukawa Lagrangian is then given by

$$\mathcal{L}_{\text{THDM}}^Y = -Y_u \bar{Q}_L i\sigma_2 \Phi_u^* u_R - Y_d \bar{Q}_L \Phi_d d_R - Y_e \bar{L}_L \Phi_e e_R + \text{h.c.}, \quad (1)$$

where $\Phi_{u,d,e}$ are Φ_1 or Φ_2 . The two doublet fields can be parameterized as

$$\Phi_i = \begin{bmatrix} w_i^+ \\ \frac{1}{\sqrt{2}}(v_i + h_i + iz_i) \end{bmatrix}, \quad (i = 1, 2), \quad (2)$$

where v_1 and v_2 are the vacuum expectation values (VEVs) for Φ_1 and Φ_2 , which satisfy $v \equiv \sqrt{v_1^2 + v_2^2} = (\sqrt{2}G_F)^{-1/2}$. The ratio of the two VEVs is defined as $\tan \beta = v_2/v_1$.

The mass eigenstates for the scalar bosons are obtained by the following orthogonal transfor-

mations as

$$\begin{aligned} \begin{pmatrix} w_1^\pm \\ w_2^\pm \end{pmatrix} &= R(\beta) \begin{pmatrix} G^\pm \\ H^\pm \end{pmatrix}, \quad \begin{pmatrix} z_1 \\ z_2 \end{pmatrix} = R(\beta) \begin{pmatrix} G^0 \\ A \end{pmatrix}, \quad \begin{pmatrix} h_1 \\ h_2 \end{pmatrix} = R(\alpha) \begin{pmatrix} H \\ h \end{pmatrix}, \\ \text{with } R(\theta) &= \begin{pmatrix} \cos \theta & -\sin \theta \\ \sin \theta & \cos \theta \end{pmatrix}, \end{aligned} \quad (3)$$

where G^\pm and G^0 are the Nambu-Goldstone bosons absorbed by the longitudinal component of W^\pm and Z , respectively. As the physical degrees of freedom, we have a pair of singly-charged Higgs boson H^\pm , a CP-odd Higgs boson A and two CP-even Higgs bosons h and H . We define h as the SM-like Higgs boson with the mass of about 126 GeV.

The Higgs potential under the softly broken Z_2 symmetry and the CP invariance is given by

$$\begin{aligned} V_{\text{THDM}} &= m_1^2 |\Phi_1|^2 + m_2^2 |\Phi_2|^2 - m_3^2 (\Phi_1^\dagger \Phi_2 + \text{h.c.}) \\ &+ \frac{1}{2} \lambda_1 |\Phi_1|^4 + \frac{1}{2} \lambda_2 |\Phi_2|^4 + \lambda_3 |\Phi_1|^2 |\Phi_2|^2 + \lambda_4 |\Phi_1^\dagger \Phi_2|^2 + \frac{1}{2} \lambda_5 \left[(\Phi_1^\dagger \Phi_2)^2 + \text{h.c.} \right]. \end{aligned} \quad (4)$$

Eight parameters in the potential are translated into eight physical parameters; namely, the masses of h , H , A and H^\pm , two mixing angles α and β appearing in Eq. (3), the VEV v and the remaining parameter M^2 defined by

$$M^2 = \frac{m_3^2}{\sin \beta \cos \beta}, \quad (5)$$

which describes the soft breaking scale of the Z_2 symmetry. Exact formulae for the Higgs boson masses and the mixing angle α are given in Ref. [26].

The Yukawa interactions are expressed in terms of mass eigenstates of the Higgs bosons as

$$\begin{aligned} \mathcal{L}_{\text{THDM}}^Y &= - \sum_{f=u,d,e} \frac{m_f}{v} \left(\xi_h^f \bar{f} f h + \xi_H^f \bar{f} f H - i \xi_A^f \bar{f} \gamma_5 f A \right) \\ &+ \left[\frac{\sqrt{2} V_{ud}}{v} \bar{u} \left(m_u \xi_A^u P_L + m_d \xi_A^d P_R \right) d H^+ + \frac{\sqrt{2} m_\ell \xi_A^e}{v} \bar{\nu} P_R e H^+ + \text{h.c.} \right], \end{aligned} \quad (6)$$

where the factors ξ_φ^f are listed in Table I.

We here summarize the tree level scale factors of h for the hVV ($V = W, Z$) and $h\bar{f}f$ couplings, which are defined by the value of the coupling constants divided by the corresponding SM values

	$\delta\xi_h^u$	$\delta\xi_h^d$	$\delta\xi_h^e$
Type-I	$-\frac{\cos\alpha}{\sin\beta}(\cot\beta\delta\beta + \tan\alpha\delta\alpha)$	$-\frac{\cos\alpha}{\sin\beta}(\cot\beta\delta\beta + \tan\alpha\delta\alpha)$	$-\frac{\cos\alpha}{\sin\beta}(\cot\beta\delta\beta + \tan\alpha\delta\alpha)$
Type-II	$-\frac{\cos\alpha}{\sin\beta}(\cot\beta\delta\beta + \tan\alpha\delta\alpha)$	$-\frac{\sin\alpha}{\cos\beta}(\tan\beta\delta\beta + \cot\alpha\delta\alpha)$	$-\frac{\sin\alpha}{\cos\beta}(\tan\beta\delta\beta + \cot\alpha\delta\alpha)$
Type-X	$-\frac{\cos\alpha}{\sin\beta}(\cot\beta\delta\beta + \tan\alpha\delta\alpha)$	$-\frac{\cos\alpha}{\sin\beta}(\cot\beta\delta\beta + \tan\alpha\delta\alpha)$	$-\frac{\sin\alpha}{\cos\beta}(\tan\beta\delta\beta + \cot\alpha\delta\alpha)$
Type-Y	$-\frac{\cos\alpha}{\sin\beta}(\cot\beta\delta\beta + \tan\alpha\delta\alpha)$	$-\frac{\sin\alpha}{\cos\beta}(\tan\beta\delta\beta + \cot\alpha\delta\alpha)$	$-\frac{\cos\alpha}{\sin\beta}(\cot\beta\delta\beta + \tan\alpha\delta\alpha)$

TABLE II: The counter term for the mixing factors in Yukawa interactions.

as follows

$$\kappa_V = \sin(\beta - \alpha) \equiv \sqrt{1 - \delta} \quad (0 \leq \delta \leq 1) \text{ for all types,} \quad (7)$$

$$\kappa_u = \xi_h^u \simeq 1 + \vartheta \cot\beta\sqrt{\delta} - \frac{\delta}{2} \text{ for all types,} \quad (8)$$

$$\kappa_d = \xi_h^d \simeq 1 + \vartheta \cot\beta\sqrt{\delta} - \frac{\delta}{2} \left(1 - \vartheta \tan\beta\sqrt{\delta} - \frac{\delta}{2} \right) \text{ for Type-I,-X (Type-II,-Y),} \quad (9)$$

$$\kappa_e = \xi_h^e \simeq 1 + \vartheta \cot\beta\sqrt{\delta} - \frac{\delta}{2} \left(1 - \vartheta \tan\beta\sqrt{\delta} - \frac{\delta}{2} \right) \text{ for Type-I,-Y (Type-II,-X),} \quad (10)$$

where δ and ϑ are $\cos^2(\beta - \alpha)$ and the sign of $\cos(\beta - \alpha)$, respectively, in the THDMs. The nearly-equals in κ_f are valid in the case of $\delta \ll 1$. Clearly, when $\sin(\beta - \alpha) = 1$ (or equivalently taking $\delta = 0$) is taken, all the scale factors given in Eqs. (7)-(10) become unity, which mean all the tree level hVV and $hf\bar{f}$ couplings are getting the same value as in the SM. We then define the SM-like limit by $\sin(\beta - \alpha) \rightarrow 1$. The other Higgs bosons; namely H^\pm , A and H , should be regarded as extra Higgs bosons. As long as we discuss in the SM-like region, the squared masses of the extra Higgs bosons are given by the following form

$$m_\Phi^2 = \lambda_i v^2 + M^2, \quad \Phi = H^\pm, A, H, \quad (11)$$

where λ_i represent some combinations of the λ couplings given in Eq. (4). We note that in general, the mass formula for H is rather complicated than Eq. (11). However, when we take $\sin(\beta - \alpha) = 1$, the expression in Eq. (11) also holds for H . See Ref. [26] for the explicit formula.

III. RENORMALIZATION

In this section, we calculate one-loop corrected Yukawa couplings for the SM-like Higgs boson h in the four types of Yukawa interactions based on the on-shell renormalization scheme. For the

calculation of each diagram, we choose the 't Hooft-Feynman gauge. The renormalized hff vertex can be expressed by the following three parts,

$$\hat{\Gamma}_{hff}(p_1^2, p_2^2, q^2) = \Gamma_{hff}^{\text{tree}} + \delta\Gamma_{hff} + \Gamma_{hff}^{\text{1PI}}(p_1^2, p_2^2, q^2), \quad (12)$$

where p_1^μ and p_2^μ are the incoming momenta for the fermion and anti-fermion, and $q^\mu (= p_1^\mu + p_2^\mu)$ is the outgoing momentum for h . In Eq. (12), the first, second and third terms in the right hand side are the contributions from the tree level diagram, the counter terms and the 1PI diagrams to the hff couplings, respectively. The tree level contribution is obtained in terms of the mixing factor listed in Table I.

The counter term contribution is given by

$$\delta\Gamma_{hff} = -i\frac{m_f}{v}\xi_h^f \left[\frac{\delta m_f}{m_f} + \delta Z_V^f + \frac{1}{2}\delta Z_h + \frac{\delta\xi_h^f}{\xi_h^f} + \frac{\xi_H^f}{\xi_h^f}(\delta C_h + \delta\alpha) - \frac{\delta v}{v} \right], \quad (13)$$

where $\delta\xi_h^f$ depend on the type of Yukawa interaction, which are listed in Table II. In the following, we explain how each of the counter terms in Eq. (13) can be determined. The counter terms for the fermion mass and the wave function renormalization are given by

$$m_f \rightarrow m_f + \delta m_f, \quad \psi_L \rightarrow \left(1 + \frac{1}{2}\delta Z_L^f\right)\psi_L, \quad \psi_R \rightarrow \left(1 + \frac{1}{2}\delta Z_R^f\right)\psi_R, \quad (14)$$

where ψ_L and ψ_R are the left-handed and right-handed fermions. The renormalized fermion two point function is expressed by the following two parts;

$$\hat{\Pi}_{ff}(p^2) = \hat{\Pi}_{ff,V}(p^2) + \hat{\Pi}_{ff,A}(p^2), \quad (15)$$

where

$$\begin{aligned} \hat{\Pi}_{ff,V}(p^2) &= \not{p} \left[\Pi_{ff,V}^{\text{1PI}}(p^2) + \delta Z_V^f \right] + m_f \left[\Pi_{ff,S}^{\text{1PI}}(p^2) - \delta Z_V^f - \frac{\delta m_f}{m_f} \right], \\ \hat{\Pi}_{ff,A}(p^2) &= -\not{p}\gamma_5 \left[\Pi_{ff,A}^{\text{1PI}}(p^2) + \delta Z_A^f \right], \end{aligned} \quad (16)$$

with

$$\delta Z_V^f = \frac{\delta Z_L^f + \delta Z_R^f}{2}, \quad \delta Z_A^f = \frac{\delta Z_L^f - \delta Z_R^f}{2}. \quad (17)$$

In Eq. (16), $\Pi_{ff,V}^{\text{1PI}}$, $\Pi_{ff,A}^{\text{1PI}}$ and $\Pi_{ff,S}^{\text{1PI}}$ are the vector, axial vector and scalar parts of the 1PI diagram contributions at the one-loop level, respectively. By imposing the three renormalization conditions

$$\begin{aligned} \hat{\Pi}_{ff,V}(m_f^2) &= 0, \\ \frac{d}{d\not{p}}\hat{\Pi}_{ff,V}(p^2)\Big|_{p^2=m_f^2} &= 0, \quad \frac{d}{d\not{p}}\hat{\Pi}_{ff,A}(p^2)\Big|_{p^2=m_f^2} = 0, \end{aligned} \quad (18)$$

we obtain

$$\begin{aligned}
\frac{\delta m_f}{m_f} &= \Pi_{ff,V}^{1\text{PI}}(m_f^2) + \Pi_{ff,S}^{1\text{PI}}(m_f^2), \\
\delta Z_V^f &= -\Pi_{ff,V}^{1\text{PI}}(m_f^2) - 2m_f^2 \left[\frac{d}{dp^2} \Pi_{ff,V}^{1\text{PI}}(p^2) \Big|_{p^2=m_f^2} + \frac{d}{dp^2} \Pi_{ff,S}^{1\text{PI}}(p^2) \Big|_{p^2=m_f^2} \right], \\
\delta Z_A^f &= -\Pi_{ff,A}^{1\text{PI}}(m_f^2) + 2m_f^2 \frac{d}{dp^2} \Pi_{ff,A}^{1\text{PI}}(p^2) \Big|_{p^2=m_f^2}.
\end{aligned} \tag{19}$$

Although the counter term δZ_A^f is not used in the following discussion, we here show the expression for completeness.

According to Ref. [26], the counter terms δZ_h , δC_h and $\delta\alpha$ are defined in the CP-even Higgs sector as

$$\begin{pmatrix} H \\ h \end{pmatrix} \rightarrow \begin{pmatrix} 1 + \frac{1}{2}\delta Z_H & \delta C_h + \delta\alpha \\ \delta C_h - \delta\alpha & 1 + \frac{1}{2}\delta Z_h \end{pmatrix} \begin{pmatrix} H \\ h \end{pmatrix}. \tag{20}$$

In order to determine them, we impose the on-shell conditions for the scalar two point functions;

$$\frac{d}{dp^2} \hat{\Pi}_{hh}(p^2) \Big|_{p^2=m_h^2} = 0, \quad \hat{\Pi}_{Hh}(p^2 = m_H^2) = \hat{\Pi}_{Hh}(p^2 = m_h^2) = 0, \tag{21}$$

where $\hat{\Pi}_{hh}$ and $\hat{\Pi}_{Hh}$ are the renormalized two point functions of hh and Hh . From the three conditions given in Eq. (21), three counter terms δZ_h , $\delta\alpha$ and δC_h are determined.

The counter term $\delta\beta$, which is defined by the shift $\beta \rightarrow \beta + \delta\beta$, is determined by requiring that the mixing between A and G^0 is absent at the on-shell for A and G^0 . This can be expressed in terms of the renormalized A - G^0 mixing $\hat{\Pi}_{AG}$ as

$$\hat{\Pi}_{AG}(p^2 = m_Z^2) = \hat{\Pi}_{AG}(p^2 = m_A^2) = 0. \tag{22}$$

In fact, we can determine not only $\delta\beta$ but also the counter term associated with the mixing between the CP-odd states δC_A corresponding to δC_h in the CP-even sector.

We here note that the condition given in Eq. (22) with $p^2 = m_A^2$ is equivalent to the requirement for the vanishing Z - A mixing due to the Ward-Takahashi identity; i.e.,

$$\hat{\Pi}_{ZA}(p^2 = m_A^2) = 0, \tag{23}$$

where $\hat{\Pi}_{ZA}$ is defined from the renormalized Z - A mixing $\hat{\Pi}_{ZA}^\mu = -ip^\mu \hat{\Pi}_{ZA}$. According to Ref. [27], the determination of $\delta\beta$ by Eq. (22) or (23) has a gauge dependence of order m_Z^2/m_A^2 . We neglect such a dependence in the following discussion, because it is not essentially important in our numerical results.

The counter term for the VEV δv is determined from the renormalization of the electroweak parameters. We determine the counter terms for the masses of W and Z bosons and the fine structure constant according to the electroweak on-shell scheme [28], so that we obtain

$$\frac{\delta v}{v} = \frac{1}{2} \left[\frac{s_W^2 - c_W^2}{s_W^2} \frac{\Pi_{WW}^{1\text{PI}}(m_W^2)}{m_W^2} + \frac{c_W^2}{s_W^2} \frac{\Pi_{ZZ}^{1\text{PI}}(m_Z^2)}{m_Z^2} - \frac{d}{dp^2} \Pi_{\gamma\gamma}^{1\text{PI}}(p^2) \Big|_{p^2=0} + \frac{2s_W}{c_W} \frac{\Pi_{Z\gamma}^{1\text{PI}}(0)}{m_Z^2} \right], \quad (24)$$

where $\Pi_{XY}^{1\text{PI}}$ are the contributions from the 1PI diagrams for the gauge boson self-energies and $c_W = \cos \theta_W$ and $s_W = \sin \theta_W$ with θ_W being the weak mixing angle. Instead of the calculation of $\frac{d}{dp^2} \Pi_{\gamma\gamma}^{1\text{PI}}(p^2) \Big|_{p^2=0}$, we introduce the shift of the fine structure constant α_{em} from 0 to the scale of m_Z as

$$\Delta\alpha_{\text{em}} = \frac{d}{dp^2} \Pi_{\gamma\gamma}^{1\text{PI}}(p^2) \Big|_{p^2=0} - \frac{d}{dp^2} \Pi_{\gamma\gamma}^{1\text{PI}}(p^2) \Big|_{p^2=m_Z^2}. \quad (25)$$

Finally, the 1PI contributions to the $hff\bar{f}$ vertex can be decomposed into the following eight form factors in general;

$$\Gamma_{hff}^{1\text{PI}}(p_1^2, p_2^2, q^2) = F_{hff}^S + \gamma_5 F_{hff}^P + \not{p}_1 F_{hff}^{V1} + \not{p}_2 F_{hff}^{V2} + \not{p}_1 \gamma_5 F_{hff}^{A1} + \not{p}_2 \gamma_5 F_{hff}^{A2} + \not{p}_1 \not{p}_2 F_{hff}^T + \not{p}_1 \not{p}_2 \gamma_5 F_{hff}^{PT}. \quad (26)$$

We note that in the on-shell case; i.e., $p_1^2 = p_2^2 = m_f^2$, the form factors proportional to γ_5 are vanished in the SM-like limit, so that only F_{hff}^S , F_{hff}^{V1} , F_{hff}^{V2} and F_{hff}^T are survived. Among those form factors, F_{hff}^S gives the dominant contribution to the $hff\bar{f}$ vertex.

We show the expression of the deviation in renormalized Yukawa coupling from the SM prediction. Because the general expression is rather complicated, we here give the formula in the case of $\sin(\beta - \alpha) = 1$ and $m_{H^+} = m_A = m_H$ ($\equiv m_\Phi$) in terms of the Passarino-Veltman functions [29];

$$\begin{aligned} & \hat{\Gamma}_{hff}^{\text{THDM}}(m_f^2, m_f^2, m_h^2) \\ & \simeq \hat{\Gamma}_{hff}^{\text{SM}}(m_f^2, m_f^2, m_h^2) + \frac{m_f}{v} \frac{1}{16\pi^2} \left\{ \frac{2m_{f'}^2}{v^2} \xi_A^d \cot \beta \left[(m_h^2 - 2m_{f'}^2) C_{12}(m_{f'}, m_\Phi, m_{f'}) \right. \right. \\ & \left. \left. + (2m_{f'}^2 - m_f^2) C_0(m_{f'}, m_\Phi, m_{f'}) + v \lambda_{\Phi\Phi h} C_0(m_\Phi, m_{f'}, m_\Phi) \right] \right. \\ & \left. + 4\lambda_{\Phi\Phi h}^2 \frac{d}{dp^2} B_0(p^2; m_\Phi, m_\Phi) \Big|_{p^2=m_h^2} - \frac{6m_t^2}{v^2} I_f \xi_A^f \cot \beta B_0(m_\Phi^2; m_t, m_t) \right. \\ & \left. + \frac{6m_t^4}{v^2(m_\Phi^2 - m_h^2)} I_f \xi_A^f \cot \beta \left[\left(4 - \frac{m_h^2}{m_t^2} \right) B_0(m_h^2; m_t, m_t) - \left(4 - \frac{m_\Phi^2}{m_t^2} \right) B_0(m_\Phi^2; m_t, m_t) \right] \right. \\ & \left. + \frac{6\lambda_{\Phi\Phi h} \lambda_{\Phi\Phi H}}{m_\Phi^2 - m_h^2} I_f \xi_A^f \left[B_0(m_h^2; m_\Phi, m_\Phi) - B_0(m_\Phi^2; m_\Phi, m_\Phi) \right] \right\}, \quad (27) \end{aligned}$$

where f' is the fermion whose electromagnetic charge is different by one unit from f , and $I_f = +1/2$ ($-1/2$) for $f = u$ (d, e). The scalar three-point couplings are given by

$$\lambda_{\Phi\Phi h} = \frac{m_h^2 + 2m_\Phi^2 - 2M^2}{v}, \quad \lambda_{\Phi\Phi H} = \frac{M^2 - m_\Phi^2}{v} \cot 2\beta. \quad (28)$$

The shortened notations are used such as $C_i(m_f^2, m_f^2, m_h^2; m_1, m_2, m_3) = C_i(m_1, m_2, m_3)$ in Eq. (27). We will give the full one-loop expression in the general case elsewhere [30].

IV. RESULTS

In this section, we show the numerical results. We use the following inputs [6];

$$\begin{aligned} m_Z &= 91.1875 \text{ GeV}, \quad G_F = 1.16639 \times 10^{-5} \text{ GeV}^{-2}, \quad \alpha_{\text{em}}^{-1} = 137.035989, \quad \Delta\alpha_{\text{em}} = 0.06635, \\ m_t &= 173.07 \text{ GeV}, \quad m_b = 4.66 \text{ GeV}, \quad m_c = 1.275 \text{ GeV}, \quad m_\tau = 1.77684 \text{ GeV}. \end{aligned} \quad (29)$$

We here take all the extra Higgs boson masses to be the same; i.e., $m_{H^+} = m_A = m_H$ ($= m_\Phi$) for avoiding the constraint from the electroweak rho parameter [7]. In the THDM, theoretical bounds from perturbative unitarity and vacuum stability have been derived in Refs. [31] and [32], respectively, and we take into account them using formulae given in Ref. [26]. We will show more comprehensive choice of parameters elsewhere [30].

We evaluate the one-loop renormalized scale factors defined by

$$\hat{\kappa}_f \equiv \frac{\hat{\Gamma}_{hff}(m_f^2, m_f^2, m_h^2)_{\text{THDM}}}{\hat{\Gamma}_{hff}(m_f^2, m_f^2, m_h^2)_{\text{SM}}}, \quad \text{for } f = c, b, \tau, \quad (30)$$

where

$$\hat{\Gamma}_{hff}(m_f^2, m_f^2, m_h^2) = \Gamma_{hff}^{\text{tree}} + \delta\Gamma_{hff} + F_S(m_f^2, m_f^2, m_h^2). \quad (31)$$

Only for the top Yukawa coupling, the momentum assignment given in Eq. (30) is not kinematically allowed, so that we assign the external momenta by $p_1^2 = m_t^2$, $p_2^2 = (m_t + m_h)^2$ and $q^2 = m_h^2$ so as to be the on-shell top-quark and the Higgs boson, which is related to the process; $e^+e^- \rightarrow t^*\bar{t} \rightarrow t\bar{t}h$.

In Fig. 1, we first show the decoupling behavior of the one-loop contributions to the hff couplings. As an example to see the decoupling, we only show the case with $\lambda_i v^2 = (300 \text{ GeV})^2$ (see Eq. (11)) which corresponds to the case where the value of M^2 is changed to keep the relation $(300 \text{ GeV})^2 = m_\Phi^2 - M^2$. In this figure, the deviations in the renormalized Yukawa couplings; i.e., $\hat{\kappa}_f - 1$ for $f = b, \tau$ and c are shown as a function of m_Φ in the Type-I (upper-left), Type-II (upper-right), Type-X (lower-left) and Type-Y (lower-right) THDMs with $\sin(\beta - \alpha) = 1$. The

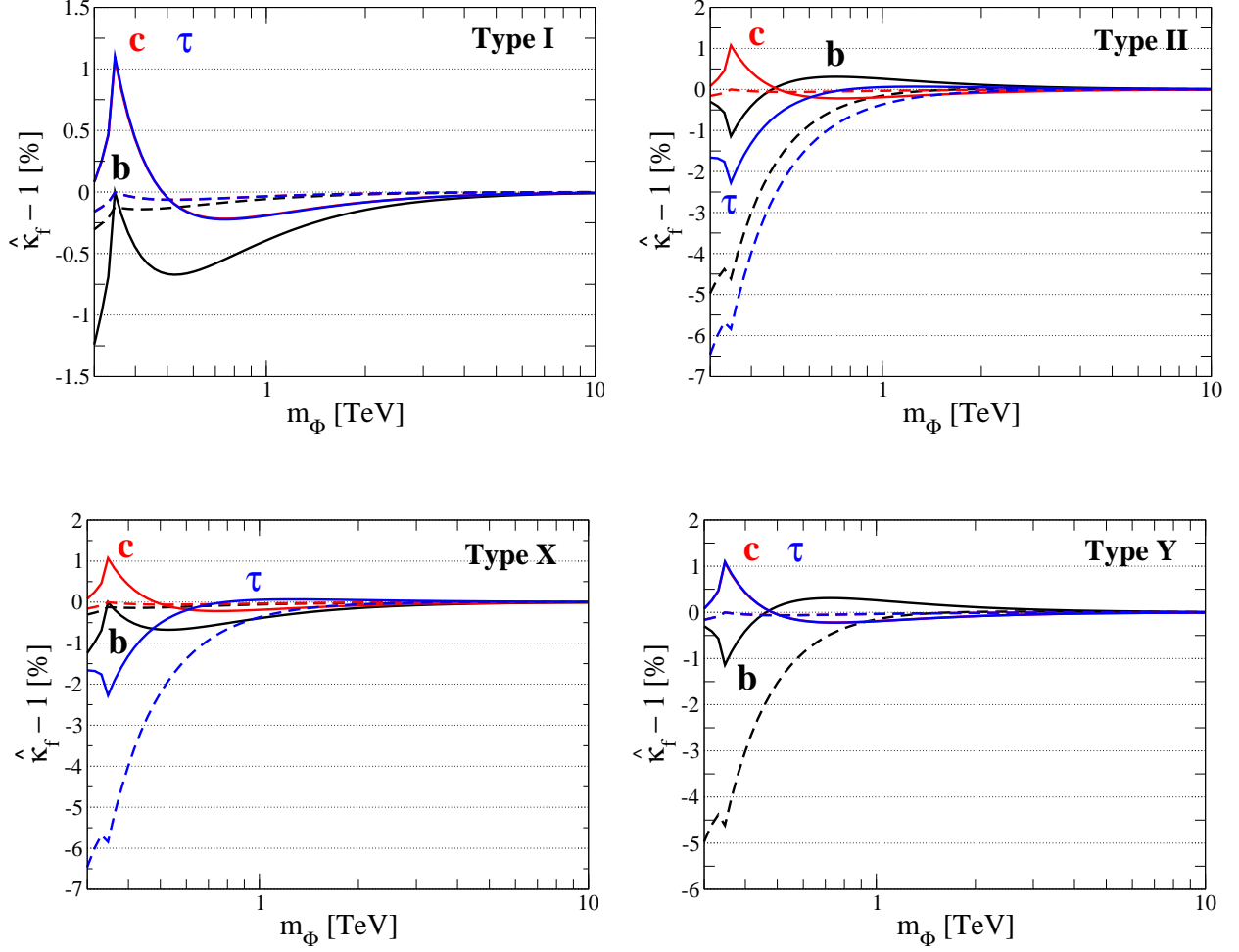


FIG. 1: Deviations in the renormalized Yukawa couplings for b , τ and c as a function of m_Φ ($= m_{H^+} = m_A = m_H$) in the case of $\sin(\beta - \alpha) = 1$ in the Type-I (upper-left), Type-II (upper-right), Type-X (lower-left) and Type-Y (lower-right) THDMs. The value of M^2 is taken so as to keep the relation $(300 \text{ GeV})^2 = m_\Phi^2 - M^2$. The solid and dashed curves are the results with $\tan\beta = 1$ and $\tan\beta = 3$, respectively.

solid and dashed curves are the results with $\tan\beta = 1$ and $\tan\beta = 3$, respectively. In the large mass region, the value of $\hat{\kappa}_f - 1$ asymptotically approaches to 0 suggesting that the effects of the extra Higgs boson loops vanish. Thus, we can verify the reproduction of the SM prediction in the large mass limit. We note that the peak at around $m_\Phi = 2m_t$ comes from the resonance of the top quark loop contribution to $\Pi_{AA}^{\text{PI}}(p^2 = m_A^2)$ which appears from the renormalization condition of $\delta\beta$.

In Fig. 2, we show the $\tan\beta$ dependence in $\hat{\kappa}_f$ for $f = b, \tau$ and c in the Type-I (upper-left), Type-II (upper-right), Type-X (lower-left) and Type-Y (lower-right) THDMs with $\sin(\beta - \alpha) = 1$.

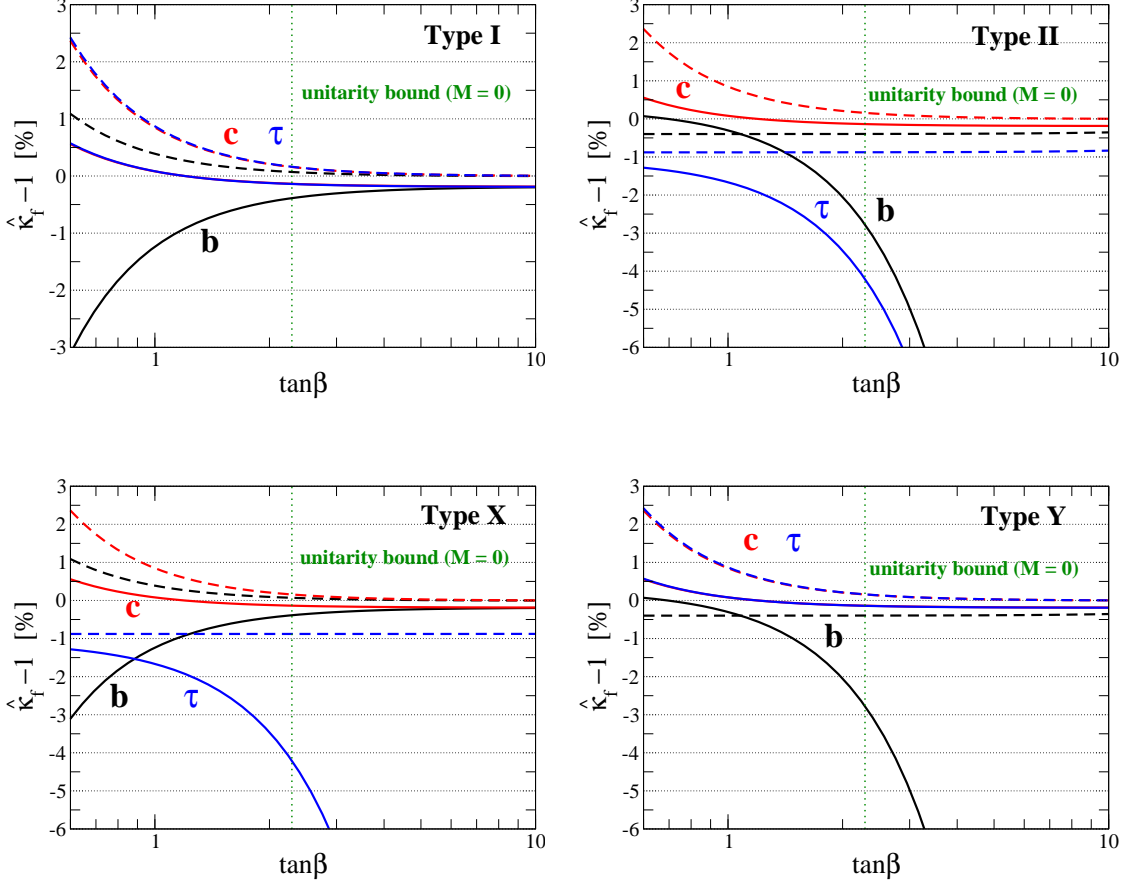


FIG. 2: Deviations in the renormalized Yukawa couplings for b , τ and c as a function of $\tan\beta$ in the case of $\sin(\beta - \alpha) = 1$ in the Type-I (upper-left), Type-II (upper-right), Type-X (lower-left) and Type-Y (lower-right) THDMs. The extra Higgs boson masses m_Φ are taken to be 300 GeV in all the plots. The solid and dashed curves are the results with $M = 0$ and 300 GeV, respectively. For the case of $M = 0$, the upper limit on $\tan\beta$ from the unitarity bound is denoted by the vertical dotted line (at around $\tan\beta \sim 2.3$).

We set the extra Higgs boson masses m_Φ to be 300 GeV and M to be 0 (solid curves) and 300 GeV (dashed curves). In the case of $M = 0$, $\tan\beta \gtrsim 2.3$ is excluded by the unitarity bound. In the Type-II THDM, the magnitude of $\hat{\kappa}_b$ and $\hat{\kappa}_\tau$ is increased as $\tan\beta$ is getting larger values because of the term proportional to $\lambda_{\Phi\Phi_h}\lambda_{\Phi\Phi_H}$ in Eq. (27). Similar behavior can be seen in $\hat{\kappa}_\tau$ ($\hat{\kappa}_b$) in the Type-X (Type-Y) THDM. In the Type-I THDM, such an enhancement does not appear because of the factor $\cot\beta$. We note that, although in Fig. 2 the results are shown for $0.6 < \tan\beta < 10$, the case of $\tan\beta < 1$ has been disfavored by the B physics experiments such as $b \rightarrow s\gamma$ and the B - \bar{B} mixing [33] in four types of Yukawa interactions.

Next, we show the nondecoupling effect due to the extra Higgs boson loops to the hff couplings.

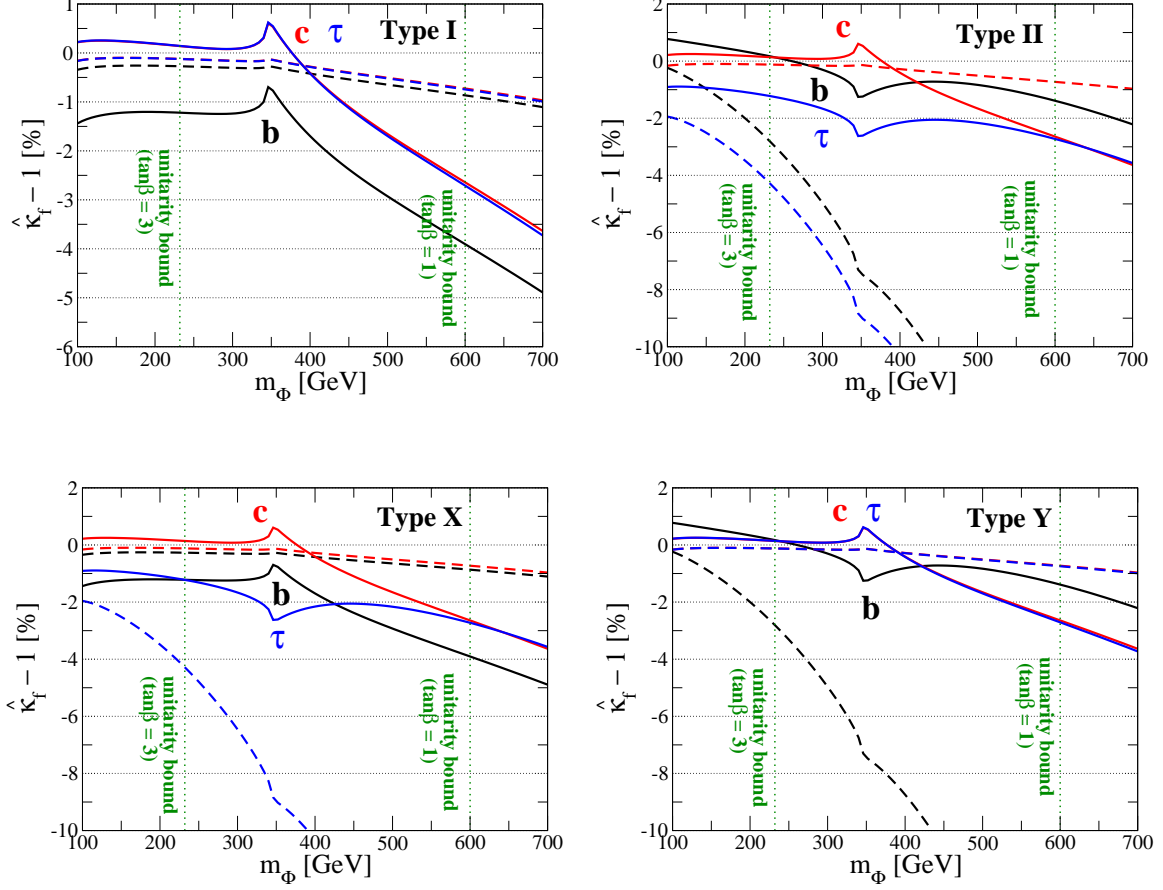


FIG. 3: Deviations in the renormalized Yukawa couplings for b , τ and c as a function of m_Φ in the case of $\sin(\beta - \alpha) = 1$ in the Type-I (upper-left), Type-II (upper-right), Type-X (lower-left) and Type-Y (lower-right) THDMs. We take $M = 0$ in all the plots. The solid and dashed curves are the results with $\tan\beta = 1$ and 3 GeV, respectively. The upper limits of m_Φ are denoted by the vertical dotted lines (at around $m_\Phi \simeq 600$ and 230 GeV for $\tan\beta = 1$ and 3 , respectively) from the unitarity bound.

Such an effect can be extracted from Eqs. (27) and (28) symbolically as;

$$\hat{\Gamma}_{hff}^{\text{THDM}} \sim \hat{\Gamma}_{hff}^{\text{SM}} + \frac{1}{16\pi^2} \frac{m_f m_\Phi^2}{v^2} \left(1 - \frac{M^2}{m_\Phi^2}\right)^2. \quad (32)$$

From the above expression, it is clarified that there appears the quadratic dependence of m_Φ . Such a quadratic dependence vanishes when $M \simeq m_\Phi$.

In Fig. 3, the m_Φ dependence in $\hat{\kappa}_f$ for $f = b, \tau$ and c is shown in the Type-I (upper-left), Type-II (upper-right), Type-X (lower-left) and Type-Y (lower-right) THDMs with $\sin(\beta - \alpha) = 1$. The solid and dashed curves are the results with $\tan\beta = 1$ and 3 , respectively. We here take

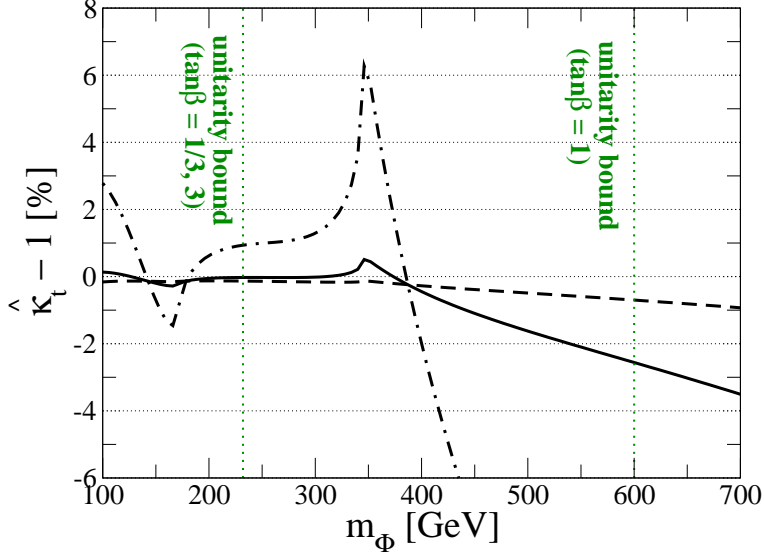


FIG. 4: Deviations in the renormalized top Yukawa couplings as a function of m_Φ in the case of $\sin(\beta-\alpha) = 1$ and $M = 0$. The dash-dotted, solid and dashed curves are the results with $\tan\beta = 1/3, 1$ and 3 , respectively. The upper limits of m_Φ are denoted by the vertical dotted lines at around $m_\Phi \simeq 600$ and (230) GeV for $\tan\beta = 1$ and $(3$ and $1/3)$, respectively from the unitarity bound.

$M^2 = 0$ to see the nondecoupling effect in all the plots.³ The maximal value of m_Φ is constrained by the unitarity bound; i.e., $m_\Phi \gtrsim 600$ GeV (230 GeV) is excluded in the case with $\tan\beta = 1$ (3) as shown by the vertical dotted lines. In the case of $\tan\beta = 1$, the maximal allowed deviations in $\hat{\kappa}_f$ are about from -2% to -5% depending on the types of Yukawa interactions.

In the above discussions, we consider Yukawa couplings for the bottom quark, charm quark and tau lepton. Let us discuss the top Yukawa coupling. As already mentioned in the beginning of this section, only the top Yukawa coupling is treated as different way from the other fermions; namely, $\hat{\kappa}_t$ is defined by

$$\hat{\kappa}_t \equiv \frac{\hat{\Gamma}_{htt}(m_t^2, (m_t + m_h)^2, m_h^2)_{\text{THDM}}}{\hat{\Gamma}_{htt}(m_t^2, (m_t + m_h)^2, m_h^2)_{\text{SM}}}. \quad (33)$$

In Fig. 4, deviations in the renormalized top Yukawa coupling $\hat{\kappa}_t - 1$ are shown as a function of m_Φ in the case of $\sin(\beta-\alpha) = 1$ and $M = 0$. The value of $\tan\beta$ is fixed by $1/3$ (dash-dotted)⁴, 1 (solid curve) and 3 (dashed curve). The difference in $\hat{\kappa}_t$ among the types of Yukawa interactions can be neglected similar to $\hat{\kappa}_c$. The height of the peak at around $m_\Phi = 2m_t$ depends on $\cot^2\beta$, so that we

³ if we take negative values for M^2 , larger nondecoupling effects can be obtained as compared to the case with $M^2 = 0$. However, too large negative values for M^2 are easily excluded by perturbative unitarity.

⁴ As we already mentioned before, the case of $\tan\beta = 1/3$ has been excluded by the B physics data. Nevertheless, we show the case with $\tan\beta = 1/3$ just for the reference.

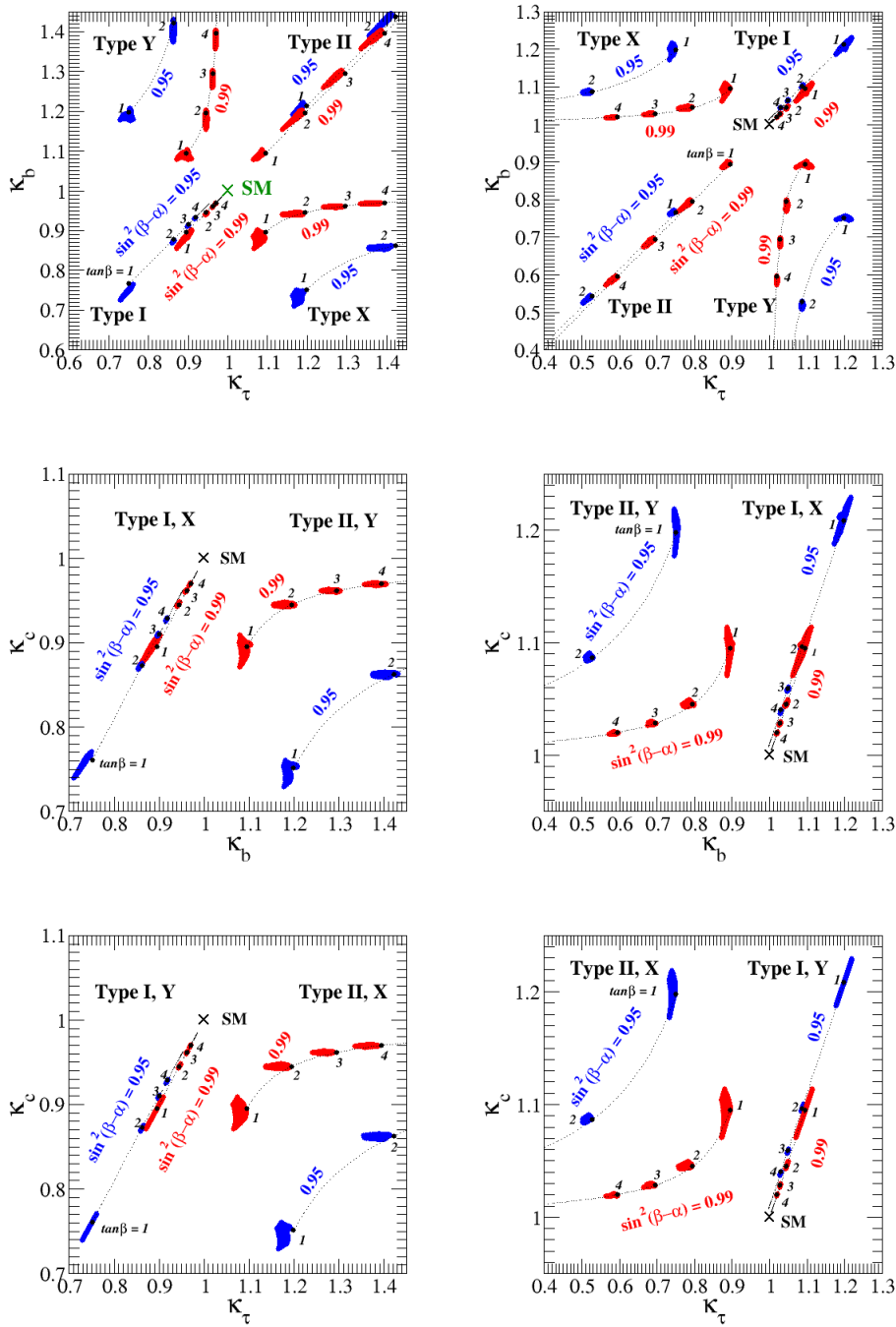


FIG. 5: Predictions of various scale factors on the κ_τ vs κ_b (upper panels), κ_b vs κ_c (middle panels) and κ_τ vs κ_c (bottom panels) planes in four types of Yukawa interactions. The left and right three figures show the cases with $\cos(\beta - \alpha) < 0$ and $\cos(\beta - \alpha) > 0$, respectively. Each black dot shows the tree level result with $\tan\beta=1, 2, 3$ and 4 . One-loop corrected results are indicated by red for $\sin^2(\beta - \alpha) = 0.99$ and blue for $\sin^2(\beta - \alpha) = 0.95$ regions where m_Φ and M are scanned over from 100 GeV to 1 TeV and 0 to m_Φ , respectively. All the plots are allowed by the unitarity and vacuum stability bounds.

can see the large peak in the case of $\tan\beta = 1/3$. The maximal allowed amount for the deviation

in the top Yukawa coupling is about +4 %, -6 % and -1 % for the cases with $\tan\beta = 1/3, 1$ and 3, respectively.

Finally, we show the one-loop results for the Yukawa couplings in the planes of fermion scale factors. In Fig. 5, predictions of various scale factors are shown on the κ_τ vs κ_b (upper panels), κ_b vs κ_c (middle panels) and κ_τ vs κ_c (bottom panels) planes. When we consider the case with $\sin(\beta - \alpha) \neq 1$, the sign dependence of $\cos(\beta - \alpha)$ to $\hat{\kappa}_f$ is also important as we can see Eqs. (8), (9) and (10). Thus, we show the both cases with $\cos(\beta - \alpha) < 0$ (left panels) and $\cos(\beta - \alpha) > 0$ (right panels). The value of $\tan\beta$ is discretely taken as $\tan\beta=1, 2, 3$ and 4. The tree level predictions are indicated by the black dots, while the one-loop corrected results are shown by the red for $\sin^2(\beta - \alpha) = 0.99$ and blue for $\sin^2(\beta - \alpha) = 0.95$ regions where the values of m_Φ and M are scanned over from 100 GeV to 1 TeV and 0 to m_Φ , respectively. All the plots are allowed by the unitarity and vacuum stability bounds.

The tree level behaviors on κ - κ panels can be understood by looking at the expressions given in Eqs. (8), (9) and (10). In the middle and bottom panels, predictions in two of four THDMs are degenerate at the tree level; e.g., results in the Type-I and Type-X THDMs are the same on the κ_b - κ_c panel. This is because the same Higgs doublet field couples to corresponding fermions, which can be understood more clearly by looking at the expression given in Eqs. (8), (9) and (10). On the other hand, in the κ_τ - κ_b plane, predictions in all the four types are located in different areas with each other. Thus, all the types of THDMs give different predictions by looking at all three combinations of κ - κ planes.

Even when we take into account the one-loop corrections to the Yukawa couplings, this behavior; i.e., predictions are well separated among the four types of THDMs, does not so change as we see the red and blue colored regions. Therefore, we conclude that all the THDMs can be distinguished from each other by measuring the charm, bottom and tau Yukawa couplings precisely when the gauge couplings hVV are deviated from the SM prediction with $\mathcal{O}(1)\%$.

We here comment on the hVV couplings in the THDMs. Although the tree level deviations in the hVV couplings are described by the factor $\sin(\beta - \alpha)$, these values can be modified at the one-loop level. In Ref. [26], the one-loop corrected hZZ vertex has been calculated in the softly-broken Z_2 symmetric THDM. It has been found that for the fixed value of $\sin(\beta - \alpha)$, the one-loop corrections to the hZZ vertex are less than 1% even taking the maximal nondecoupling case.

Before the conclusions, we mention about the expected accuracy for the various Higgs boson couplings measured at future colliders such as the LHC with the 14 TeV run and the ILC. According to the ILC Technical Design Report [3, 4], the hVV couplings are expected to be measured with

about 4% accuracy at the LHC with 300 fb^{-1} . The accuracy for the $ht\bar{t}$, $hb\bar{b}$ and $h\tau\tau$ couplings are supposed to be about 16%, 14% and 11%, respectively. At the ILC250 (ILC500) where the collision energy and the integrated luminosity are 250 GeV (500 GeV) and 250 fb^{-1} (500 fb^{-1}) combining with the results assuming 300 fb^{-1} at the LHC, the hWW and hZZ couplings are expected to be measured by about 1.9% (0.2%) and about 0.4% (0.3%), respectively. The $hc\bar{c}$, $hb\bar{b}$ and $h\tau\tau$ couplings are supposed to be measured by about 5.1% (2.6%), 2.8% (1.0%) and 3.3% (1.8%) at the ILC250 (ILC500). For the $ht\bar{t}$ coupling, it will be measured with 12.0% and 9.6% accuracy at the ILC250 and ILC500, respectively. Therefore, if $\mathcal{O}(1)\%$ deviations in the hVV couplings from the SM values are established at the ILC250, we can compare the predictions of $\hat{\kappa}_f$ to the corresponding measured values at the ILC500, which are typically measured by $\mathcal{O}(1)\%$. We can then discriminate the types of Yukawa interactions in the THDM.

V. CONCLUSIONS

We have evaluated radiative corrections to the $hf\bar{f}$ couplings in the THDMs with the softly-broken Z_2 symmetry. We have found that one-loop contributions of extra Higgs bosons can modify the $hf\bar{f}$ couplings to be maximally about 5% under the constraint from perturbative unitarity and vacuum stability. The results indicate that the pattern of tree-level deviations by the mixing effect in each type of Yukawa couplings from the SM predictions does not change even including radiative corrections. Moreover, when the gauge couplings hVV will be found to be slightly (with a percent level) differ from the SM predictions, the $hf\bar{f}$ couplings also deviate but more largely. In this case, by comparing the predictions with precisely measured $hf\bar{f}$ and hVV couplings at the ILC, we can determine the type of Yukawa couplings and also can obtain information on the extra Higgs bosons, even when they are not found directly.

Acknowledgments

S.K. was supported in part by Grant-in-Aid for Scientific Research, Japan Society for the Promotion of Science (JSPS), Nos. 22244031 and 24340046, and The Ministry of Education, Culture, Sports, Science and Technology (MEXT), No. 23104006. M.K. was supported in part by JSPS, No. K2510031. K.Y. was supported in part by the National Science Council of R.O.C.

under Grant No. NSC-101-2811-M-008-014.

- [1] G. Aad *et al.*, [ATLAS Collaboration], Phys. Lett. B **716**, 1 (2012); S. Chatrchyan *et al.*, [CMS Collaboration], Phys. Lett. B **716**, 30 (2012).
- [2] M. E. Peskin, arXiv:1207.2516 [hep-ph].
- [3] D. M. Asner, *et al.*, arXiv:1310.0763 [hep-ph].
- [4] H. Baer, *et al.*, arXiv:1306.6352 [hep-ph].
- [5] M. Klute, R. Lafaye, T. Plehn, M. Rauch and D. Zerwas, Europhys. Lett. **101**, 51001 (2013).
- [6] J. Beringer *et al.* (Particle Data Group), Phys. Rev. D **86**, 010001 (2012).
- [7] D. Toussaint, Phys. Rev. D **18**, 1626 (1978); S. Bertolini, Nucl. Phys. B **272**, 77 (1986); M. E. Peskin and J. D. Wells, Phys. Rev. D **64**, 093003 (2001); W. Grimus, L. Lavoura, O. M. Ogreid and P. Osland, Nucl. Phys. B **801**, 81 (2008); S. Kanemura, Y. Okada, H. Taniguchi and K. Tsumura, Phys. Lett. B **704**, 303 (2011).
- [8] T. Blank and W. Hollik, Nucl. Phys. B **514**, 113 (1998); M. C. Chen, S. Dawson and T. Krupovnickas, Phys. Rev. D **74**, 035001 (2006); P. H. Chankowski, S. Pokorski and J. Wagner, Eur. Phys. J. C **50**, 919 (2007); S. Kanemura and K. Yagyu, Phys. Rev. D **85**, 115009 (2012); M. Aoki, S. Kanemura, M. Kikuchi and K. Yagyu, Phys. Rev. D **87**, 015012 (2013).
- [9] A. Zee, Phys. Lett. B **93** (1980) 389 [Erratum-ibid. B **95** (1980) 461].
- [10] E. Ma, Phys. Rev. D **73** (2006) 077301; J. Kubo, E. Ma and D. Suematsu, Phys. Lett. B **642**, 18 (2006).
- [11] M. Aoki, S. Kanemura and O. Seto, Phys. Rev. Lett. **102**, 051805 (2009); M. Aoki, S. Kanemura and O. Seto, Phys. Rev. D **80**, 033007 (2009); M. Aoki, S. Kanemura and K. Yagyu, Phys. Rev. D **83**, 075016 (2011).
- [12] Y. Kajiyama, H. Okada and K. Yagyu, JHEP **10**, 196 (2013).
- [13] E. Ma, Phys. Rev. Lett. **86**, 2502 (2001).
- [14] M. Hashimoto and S. Kanemura, Phys. Rev. D **70**, 055006 (2004) [Erratum-ibid. D **70**, 119901 (2004)].
- [15] A. E. Nelson, D. B. Kaplan and A. G. Cohen, Nucl. Phys. B **373**, 453 (1992); N. Turok and J. Zadrozny, Nucl. Phys. B **369**, 729 (1992); K. Funakubo, A. Kakuto and K. Takenaga, Prog. Theor. Phys. **91**, 341 (1994); A. T. Davies, C. D. Froggatt, G. Jenkins and R. G. Moorhouse, Phys. Lett. B **336**, 464 (1994); J. M. Cline, K. Kainulainen and A. P. Vischer, Phys. Rev. D **54**, 2451 (1996); S. Kanemura, Y. Okada and E. Senaha, Phys. Lett. B **606**, 361 (2005); L. Fromme, S. J. Huber and M. Seniuch, JHEP **0611**, 038 (2006).
- [16] G. C. Branco *et al.*, Phys. Rept. **516**, 1 (2012).
- [17] S. L. Glashow and S. Weinberg, Phys. Rev. D **15**, 1958 (1977).
- [18] R. Barbieri, L. J. Hall and V. S. Rychkov, Phys. Rev. D **74**, 015007 (2006).
- [19] V. D. Barger, J. L. Hewett and R. J. N. Phillips, Phys. Rev. D **41**, 3421 (1990); Y. Grossman, Nucl.

- Phys. B **426**, 355 (1994).
- [20] A. G. Akeroyd, Phys. Lett. B **377**, 95 (1996).
- [21] M. Aoki, S. Kanemura, K. Tsumura and K. Yagyu, Phys. Rev. D **80**, 015017 (2009).
- [22] V. Barger, H. E. Logan and G. Shaughnessy, Phys. Rev. D **79**, 115018 (2009); H. E. Logan and D. MacLennan, Phys. Rev. D **79**, 115022 (2009); H. E. Logan and D. MacLennan, Phys. Rev. D **81**, 075016 (2010); M. Aoki, R. Guedes, S. Kanemura, S. Moretti, R. Santos and K. Yagyu, Phys. Rev. D **84**, 055028 (2011); A. Arhrib, C. -W. Chiang, D. K. Ghosh and R. Santos, Phys. Rev. D **85**, 115003 (2012); S. Kanemura, K. Tsumura and H. Yokoya, Phys. Rev. D **85**, 095001 (2012).
- [23] H. S. Cheon and S. K. Kang, JHEP **1309**, 085 (2013); S. Chang, S. K. Kang, J. -P. Lee, K. Y. Lee, S. C. Park and J. Song, JHEP **1305**, 075 (2013); A. Drozd, B. Grzadkowski, J. F. Gunion and Y. Jiang, JHEP **1305**, 072 (2013); J. Chang, K. Cheung, P. -Y. Tseng and T. -C. Yuan, Phys. Rev. D **87**, no. 3, 035008 (2013); P. M. Ferreira, R. Santos, H. E. Haber and J. P. Silva, Phys. Rev. D **87**, no. 5, 055009 (2013); C. -Y. Chen and S. Dawson, Phys. Rev. D **87**, no. 5, 055016 (2013); C. -W. Chiang and K. Yagyu, JHEP **1307**, 160 (2013); B. Grinstein and P. Uttayarat, arXiv:1304.0028 [hep-ph]; B. Coleppa, F. Kling and S. Su, arXiv:1305.0002 [hep-ph]; C. -Y. Chen, S. Dawson and M. Sher, arXiv:1305.1624 [hep-ph]; S. Kanemura, K. Tsumura and H. Yokoya, arXiv:1305.5424 [hep-ph]. Y. Kajiyama, H. Okada and K. Yagyu, arXiv:1309.6234 [hep-ph].
- [24] W. Hollik and S. Penaranda, Eur. Phys. J. C **23**, 163 (2002); A. Dobado, M. J. Herrero, W. Hollik and S. Penaranda, Phys. Rev. D **66**, 095016 (2002).
- [25] J. Guasch, W. Hollik and S. Penaranda, Phys. Lett. B **515**, 367 (2001).
- [26] S. Kanemura, S. Kiyoura, Y. Okada, E. Senaha and C. P. Yuan, Phys. Lett. B **558**, 157 (2003); S. Kanemura, Y. Okada, E. Senaha and C. -P. Yuan, Phys. Rev. D **70**, 115002 (2004).
- [27] A. Freitas and D. Stockinger, Phys. Rev. D **66**, 095014 (2002).
- [28] W. F. L. Hollik, Fortsch. Phys. **38**, 165 (1990).
- [29] G. Passarino and M. J. G. Veltman, Nucl. Phys. B **160**, 151 (1979).
- [30] S. Kanemura, M. Kikuchi and K. Yagyu, in preparation.
- [31] H. Huffer and G. Pocsik, Z. Phys. C **8**, 13 (1981); J. Maalampi, J. Sirkka and I. Vilja, Phys. Lett. B **265**, 371 (1991); S. Kanemura, T. Kubota and E. Takasugi, Phys. Lett. B **313**, 155 (1993); A. G. Akeroyd, A. Arhrib and E. M. Naimi, Phys. Lett. B **490**, 119 (2000); I. F. Ginzburg and I. P. Ivanov, Phys. Rev. D **72**, 115010 (2005).
- [32] N. G. Deshpande and E. Ma, Phys. Rev. D **18**, 2574 (1978); M. Sher, Phys. Rept. **179**, 273 (1989); S. Nie and M. Sher, Phys. Lett. B **449**, 89 (1999); S. Kanemura, T. Kasai and Y. Okada, Phys. Lett. B **471**, 182 (1999).
- [33] F. Mahmoudi and O. Stal, Phys. Rev. D **81**, 035016 (2010).